Multipole plasmonic lattice solitons

Yao Kou, Fangwei Ye,* and Xianfeng Chen†

Department of Physics, The State Key Laboratory on Fiber Optic Local Area Communication Networks and Advanced Optical Communication Systems, Shanghai Jiao Tong University, Shanghai 200240, China

(Received 17 August 2011; published 29 September 2011)

We theoretically demonstrate a variety of multipole plasmonic lattice solitons, including dipoles, quadrupoles, and necklaces, in two-dimensional metallic nanowire arrays with Kerr-type nonlinearities. Such solitons feature complex internal structures with an ultracompact mode size approaching or smaller than one wavelength. Their mode sizes and the stability characteristics are studied in detail within the framework of coupled mode theory. The conditions to form and stabilize these highly confined solitons are within the experimentally achievable range.

DOI: 10.1103/PhysRevA.84.033855 PACS number(s): 42.65.Tg, 73.20.Mf, 42.82.Et, 78.67.Pt

Concentrating and manipulating light at subwavelength scales has become a major challenge facing the development of nanophotonics. While the miniaturization of conventional optical elements is impeded by the diffraction limit, surface plasmon polaritons (SPPs), the highly localized electromagnetic waves at metal-dielectric interfaces, are considered as a promising solution to break that limitation [1]. The most representative plasmonic structures include metallic nanowires [2], V-groove channels [3], and slot waveguides [4]; they have been used as basic building blocks to design different types of functional components [5,6].

In the past years, there has been growing interest in exploring nonlinear optical properties of SPPs, as they provide a possibility of active control over optical fields at the nanoscale. For example, to overcome diffraction-induced spatial expansion of the SPP wave, one can make use of nonlinear self-actions that may lead to the formation of *spatial plasmonic solitons* [7–18]. Like solitons in dielectric media, such nonlinear SPP guided waves are able to exist not only in continuous systems [7–15], but also in discrete systems [16–18]. Since the enhanced field enhancement at metal surfaces significantly strengthens the nonlinear effects, the required power to form plasmonic solitons can be significantly reduced, which, therefore, would facilitate their experimental observation and on-chip applications.

Recently, a promising structure supporting subwavelength plasmonic lattice solitons (PLSs) was proposed, which is composed of arrays of metallic nanowires embedded in Kerr-type nonlinear media [17,18]. Such a structure enables nonlinear spatial confinement in both transverse directions, so it has a potential to support richer types of higher-order plasmonic solitons with complex internal structure. In this paper, we study the existence and stability of multipole PLSs in the two-dimensional (2D) nanowire arrays, including dipoles, quadrupoles, and necklaces. We find that all these solitons feature ultrasmall mode size, which makes them candidates to be used as information carriers in the nano all-optical systems. Different from their counterparts in all-dielectric lattices, we found that the multipole PLSs are inherently unstable in the self-focusing media, but become stable in the defocusing media when their power exceeds certain values.

The geometry of the plasmonic lattice, as shown in Fig. 1, consists of a 2D array of silver nanowires embedded in a Kerr-type nonlinear background. The intensity-dependent refractive index of the background is described by $n_d = \sqrt{\varepsilon_d} = 3.5 + n_2 I$, where $n_2 = 4 \times 10^{-18}$ m^2/W (As_2S_3) is the Kerr coefficient, and the dielectric constant of silver is set to be $\varepsilon_m = -129 + 3.3i$ [19], corresponding to the wavelength of 1.55 μm. For simplicity, in the following discussions we neglect the Ohmic loss of silver, as the level of loss ($\sim$2300 cm^{-1}) can be easily compensated with the help of currently available gain media [20]. The radius and separation distance of the nanowires are fixed as $a = 40$ nm and $d = 11a$, respectively.

To analyze the soliton states in the present system, we use a developed model based on the coupled mode theory [17]. By expanding the total fields as a superposition of the fundamental transverse magnetic mode of single nanowires and employing the conjugated form of the Lorentz reciprocity theorem, the nonlinear Schrödinger equation that describes the propagation of light beam in the proposed structure is derived as

$$\begin{aligned} i\frac{d\phi_{m,n}}{dz} &+ \kappa(\phi_{m,n+1} + \phi_{m,n-1} + \phi_{m+1,n} + \phi_{m-1,n}) \\ &+ \mu(\phi_{m+1,n+1} + \phi_{m+1,n-1} + \phi_{m-1,n+1} + \phi_{m-1,n-1}) \\ &+ \gamma|\phi_{m,n}|^2\phi_{m,n} = 0. \end{aligned} \tag{1}$$

Here $\phi_{m,n}(z)$ is the normalized mode amplitude and z is the longitudinal coordinate. κ and μ represent the coupling coefficients between neighboring and next-neighboring nanowires, respectively. Under the above-mentioned geometry parameters and wavelength, the coupling coefficients are determined as $\kappa = -1.75 \times 10^4$ m^{-1} and $\mu = -1.63 \times 10^3$ m^{-1}. Note that the negative coupling coefficient is a unique property of the plasmonic waveguide arrays, which corresponds to an inverted diffraction relation. As a result, normal and anomalous diffraction of the linear SPP wave occurs separately at the edge ($|k_x| = \pi/d$, $|k_y| = \pi/d$) and center ($k_x = k_y = 0$) of the first Brillion zone. Finally, γ is the effective nonlinear coefficient, which can be either positive (self-focusing) or negative (self-defocusing), according to the type of nonlinearities of the background dielectric materials.

*fangweiye@sjtu.edu.cn
†xfchen@sjtu.edu.cn

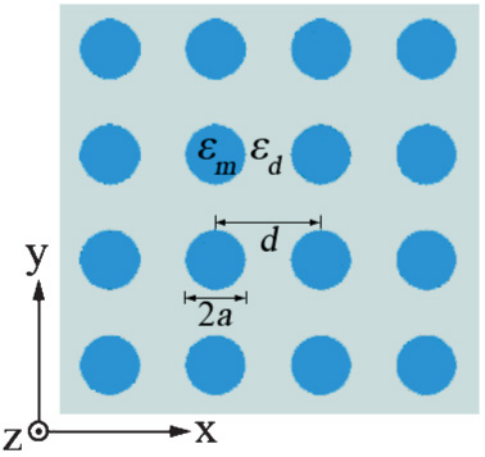

FIG. 1. (Color online) Schematic of the 2D metallic nanowire array. The nanowires of permittivity $\varepsilon_m = -129 + 3.3i$ are embedded in the nonlinear host medium with an intensity-dependent refractive index $n_d = \sqrt{\varepsilon_d} = 3.5 + n_2 I$, where $n_2 = 4 \times 10^{-18}$ m^2/W. The radius and separation distance of the nanowires are $a = 40$ nm and $d = 11a$, respectively.

We search for stationary solutions of Eq. (1) in the form $\phi_{m,n}(z) = u_{m,n} \exp(i\rho z)$, where $u_{m,n}$ is a real function independent of z and $\rho = \beta\kappa$ is the propagation constant (here β is defined as the normalized soliton wave number). Higher-order solutions are numerically found by the Newton iteration method with suitable initial conditions. Note that system (1) conserves the power $P = \sum_{m,n} |\phi_{m,n}|^2$. After solutions are found, we reconstruct the field distribution and then evaluate the soliton effective radius R using the definition $R = \{\iint |\boldsymbol{E}|^2[(x - x_0)^2 + (y - y_0)^2]dxdy / \iint |\boldsymbol{E}|^2 dxdy\}^{1/2}$, where $(x_0, y_0) = \iint (x, y)|\boldsymbol{E}|^2 dxdy / \iint |\boldsymbol{E}|^2 dxdy$ is the mean center position.

We have found a variety of multipole PLSs, including dipoles, quadrupoles, and necklaces, featuring several bright spots with a π phase difference between the neighboring ones. Such solitons can exist in both self-focusing and self-defocusing media. However, they cannot be found very close to the edge of the band gap, as these high-order modes could not have a bifurcation origin from the linear Bloch modes. Figures 2(a)–2(d) show examples of the dipole solitons comprising two bright spots at adjacent nanowires. One can see that, contrary to the case in pure-dielectric lattices, staggered and unstaggered PLSs are formed separately in the self-focusing and self-defocusing nonlinearity. This is a direct result of the inverted linear dispersion relation. Figure 2(e) plots the power of dipoles as a function of wave number β. For both staggered and unstaggered cases, $dP/d\beta$ reverses its sign at a certain point $\beta = \beta_c$, and increases almost linearly when $|\beta|$ becomes large. We found that in most of the existence domain, the spatial extent of dipoles is well confined within a subwavelength scale [Fig. 2(f)]. For example, the dipole soliton shown in Fig. 2(a) exhibits a radius of $R = 0.3\lambda$, and that corresponds to a nonlinear index change of $\Delta n = 0.02$. With increasing the power, the solitons become more localized and the radius can be compressed to $<0.2\lambda$.

Similar properties are encountered for quadrupole solitons, whose bright spots reside at four adjacent nanowires, with

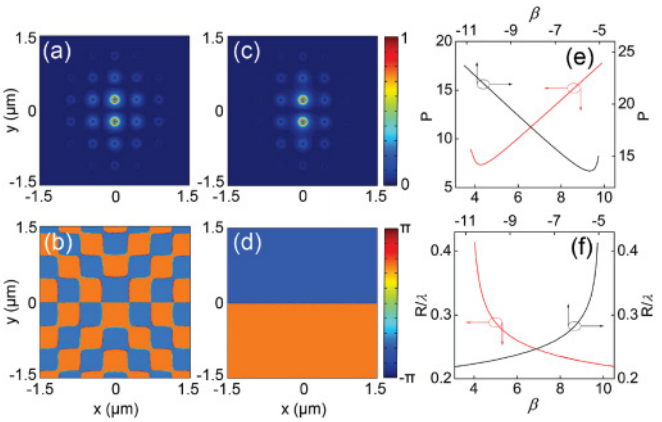

FIG. 2. (Color online) Normalized electric field amplitude [(a), (c)] and phase [(b), (d)] distribution of dipole solitons in self-focusing (left panels) and self-defocusing (middle panels) media. (a), (b) $\beta = 5.2$, $\Delta n = 0.02$. (c), (d) $\beta = -6.4$, $\Delta n = 0.04$. Right panels: Power P (e) and effective radius R (f) as a function of β.

a staggered or unstaggered phase pattern [Figs. 3(a)–3(d)]. Such solitons can be regarded as the coupled state of two parallel dipoles. The power curves resemble that of dipoles, except that for quadrupoles the power is nearly two times higher [Fig. 3(e)]. With the same change of nonlinear index, the quadrupoles also exhibit a similar spatial confinement to that of the dipoles [Fig. 3(f)].

We also found a kind of necklace soliton, comprising eight bright spots in an octagonal configuration (Fig. 4). Such solitons can be looked at as the combination of four diagonally arranged dipoles. Compared with dipoles and quadrupoles, the power of the necklaces is a monotonically increasing function of $|\beta|$ in the whole existence domain [Fig. 4(e)]. Under the same level of nonlinearity, the necklaces have a larger mode size than dipoles and quadrupoles [Fig. 4(f)]. Figure 4(a) shows a representative necklace associated with $\Delta n = 0.02$ and $R = 0.51\lambda$. It can be compressed to $R = 0.45\lambda$ with a larger index change of $\Delta n = 0.05$.

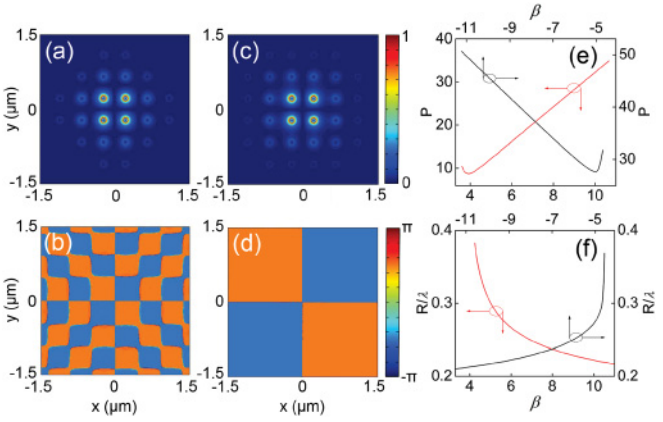

FIG. 3. (Color online) Normalized electric field amplitude [(a), (c)] and phase [(b), (d)] distribution of quadrupole solitons in self-focusing (left panels) and self-defocusing (middle panels) media. (a), (b) $\beta = 5.8$, $\Delta n = 0.02$. (c), (d) $\beta = -5.4$, $\Delta n = 0.04$. Right panels: Power P (e) and effective radius R (f) as a function of β.

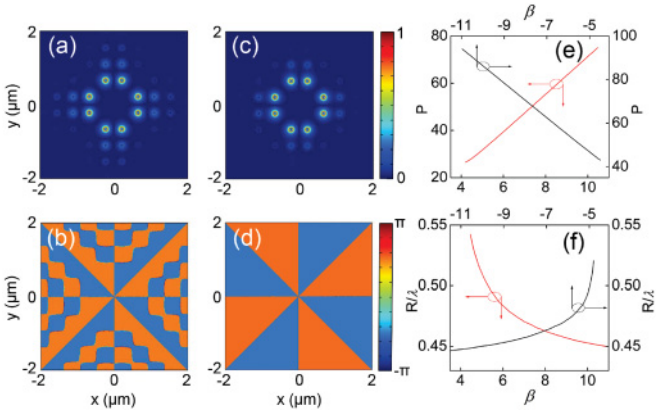

FIG. 4. (Color online) Normalized electric field amplitude [(a), (c)] and phase [(b), (d)] distribution of necklace solitons in self-focusing (left panels) and self-defocusing (middle panels) media. (a), (b) $\beta = 4.9$, $\Delta n = 0.02$. (c), (d) $\beta = -6.1$, $\Delta n = 0.04$. Right panels: Power P (e) and effective radius R (f) as a function of β.

In order to investigate the propagation stability of these higher-order PLSs, we substitute a linear perturbation with the form $\phi_{m,n} = \exp(i\rho z)[u_{m,n} + a_{m,n}\exp(-i\omega z) + b^*_{m,n}\exp(i\omega z)]$ into Eq. (1) and solve the resulting eigenvalue problem. Here $a_{m,n}$ and $b_{m,n}$ represent small perturbations on the soliton amplitudes that grow with a complex rate ω during the propagation. The stability analysis reveals that, in the self-focusing media, the (staggered) multipole PLSs are always unstable (as a nonzero imaginary part always appears in their eigenvalues ω). However, in the self-defocusing media, all the (unstaggered) multipole PLSs are found to be completely stable as long as $|\beta|$ exceeds a threshold, where the imaginary part of the eigenvalues decreases to zero (Fig. 5). This is in contrast to the case of dielectric lattices, where the solitons cannot be stable in self-defocusing media [21]. Among the three types of multipoles, the quadrupole has the highest stability threshold ($\beta = -18.2$) and therefore needs a stronger nonlinearity to stabilize its propagation, even though the corresponding nonlinear index change is found to be $\Delta n = 0.12$ and thus is still within the experimentally achievable range [22]. Note that the stability characteristics of multipole PLSs do not agree with the Vakhitov-Kolokolov criterion; the latter predicts that the solitons transform from unstable to stable state as $dP/d\beta$ changes sign from negative to positive.

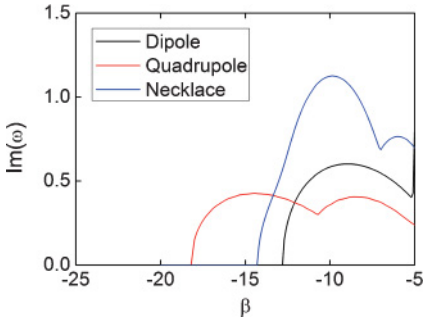

FIG. 5. (Color online) Imaginary part of perturbation growth rates versus β.

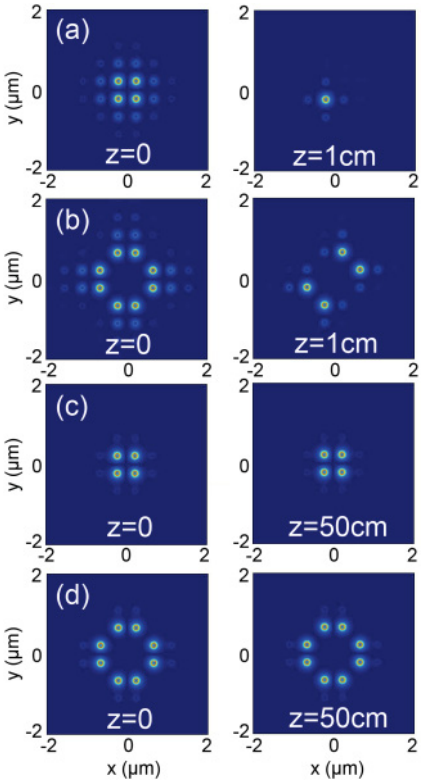

FIG. 6. (Color online) Dynamic evolution of (a) unstable quadrupole ($\beta = 5.8$), (b) unstable necklace ($\beta = 4.9$), (c) stable quadrupole ($\beta = -18.5$), and (d) stable necklace ($\beta = -15$) solitons under a 10% noise perturbation.

To confirm the results obtained by linear stability analysis and also to explore the propagation dynamics of the multipole PLSs, we finally perform direct simulations of Eq. (1) with a fourth-order Runge-Kutta method. The input conditions are the numerically found stationary soliton solutions with a 10% amplitude perturbation. As typical examples, Figs. 6(a) and 6(b) show the evolution of an unstable staggered quadrupole ($\beta = 5.8$) and a stable unstaggered quadrupole ($\beta = -18.5$), respectively. The dynamics of dipoles is found to be very similar to that of the quadrupoles, and therefore it is not shown here. One can see that when β falls in the unstable region predicted by the linear stability analysis, the original soliton structures eventually break up during their propagation. More specifically, for solitons with β approaching the band edges, their structures could totally disappear through radiating into the linear mode of a single nanowire. However, in most cases the instability makes quadrupoles decay into stable fundamental solitons [Fig. 6(a)]. Propagation simulation also confirms that, in the self-defocusing media, the quadrupoles become stable when $|\beta|$ exceeds the stability threshold [Fig. 6(c)]. Even in the unstable region, their original structures can persist for several millimeters before finally being destroyed by the growing oscillations.

An interesting unstable evolution occurs for necklaces. Simulation shows that a portion of the bright spots could survive after destruction of the initial structure [Fig. 6(b)]. These resulting structures keep quasistable propagation over very long distances, accompanied by slight breathing oscillations

in their amplitudes. Figure 6(d) also provides an example of propagation dynamics for the stable necklace. As consistent with linear stability analysis, their amplitude and phase remain unchanged after a huge propagation distance.

In conclusion, we have found a variety of multipole plasmonic lattice solitons in 2D metallic nanowire arrays with Kerr-type nonlinearities. These solitons include dipoles, quadrupoles, and necklaces, existing in both self-focusing and self-defocusing media. By means of a linear stability analysis, we found that all these solitons are unstable in the self-focusing media, but can be stable in the self-defocusing media, provided that their wave number exceeds a certain threshold. In the unstable region, they usually experience oscillation instability and finally decay into a more stable configuration after some distance of propagation. We hope that our findings may motivate the experimental observations of such ultracompact soliton structures.

This research was supported by the National Natural Science Foundation of China (Contracts No. 10874119 and No. 11104181) and the Foundation for Development of Science and Technology of Shanghai (Grant No. 10JC1407200).

[1] D. K. Gramotnev and S. I. Bozhevolnyi, Nat. Photonics **4**, 83 (2010).
[2] J. Takahara, S. Yamagishi, H. Taki, A. Morimoto, and T. Kobayashi, Opt. Lett. **22**, 475 (1997).
[3] S. I. Bozhevolnyi, V. S. Volkov, E. Devaux, and T. W. Ebbesen, Phys. Rev. Lett. **95**, 046802 (2005).
[4] J. A. Dionne, L. A. Sweatlock, H. A. Atwater, and A. Polman, Phys. Rev. B **73**, 035407 (2006).
[5] H. Ditlbacher, A. Hohenau, D. Wagner, U. Kreibig, M. Rogers, F. Hofer, F. R. Aussenegg, and J. R. Krenn, Phys. Rev. Lett. **95**, 257403 (2005).
[6] S. I. Bozhevolnyi, V. S. Volkov, E. Devaux, J. Y. Laluet, and T. W. Ebbesen, Nature **440**, 508 (2006).
[7] N. N. Akhmediev, Zh. Eksp. Teor. Fiz. **84**, 1907 (1983); V. K. Fedyanin and D. Mihalache, Z. Phys. B: Condens. Matter **47**, 167 (1982).
[8] F. Lederer and D. Mihalache, Solid State Commun. **59**, 151 (1986); D. Mihalache, D. Mazilu, and F. Lederer, Opt. Commun. **59**, 391 (1986).
[9] A. D. Boardman, A. A. Maradudin, G. I. Stegeman, T. Twardowski, and E. M. Wright, Phys. Rev. A **35**, 1159 (1987).
[10] D. Mihalache, G. I. Stegeman, C. T. Seaton, E. M. Wright, R. Zanoni, A. D. Boardman, and T. Twardowski, Opt. Lett. **12**, 187 (1987).
[11] D. Mihalache, M. Bertolotti, and C. Sibilia, Prog. Opt. **27**, 227 (1989).
[12] E. Feigenbaum and M. Orenstein, Opt. Lett. **32**, 674 (2007).
[13] A. R. Davoyan, I. V. Shadrivov, and Y. S. Kivshar, Opt. Express **17**, 21732 (2009).
[14] A. R. Davoyan, I. V. Shadrivov, A. A. Zharov, D. K. Gramotnev, and Y. S. Kivshar, Phys. Rev. Lett. **105**, 116804 (2010).
[15] A. Marini, D. V. Skryabin, and B. Malomed, Opt. Express **19**, 6616 (2011).
[16] Y. Liu, G. Bartal, D. A. Genov, and X. Zhang, Phys. Rev. Lett. **99**, 153901 (2007).
[17] F. Ye, D. Mihalache, B. Hu, and N. C. Panoiu, Phys. Rev. Lett. **104**, 106802 (2010).
[18] F. Ye, D. Mihalache, B. Hu, and N. C. Panoiu, Opt. Lett. **36**, 1179 (2011).
[19] P. B. Johnson and R. W. Christy, Phys. Rev. B **6**, 4370 (1972).
[20] N. Kirstaedter, O. G. Schmidt, N. N. Ledentsov, D. Bimberg, V. M. Ustinov, A. Y. Egorov, A. E. Zhukov, M. V. Maximov, P. S. Kopev, and Z. I. Alferov, Appl. Phys. Lett. **69**, 1226 (1996).
[21] P. G. Kevrekidis, H. Susanto, and Z. Chen, Phys. Rev. E **74**, 066606 (2006).
[22] L. Brzozowski, E. H. Sargent, A. S. Thorpe, and M. Extavour, Appl. Phys. Lett. **82**, 4429 (2003).